Quasiparticle band structure of thirteen semiconductors and insulators

Xuejun Zhu and Steven G. Louie
Department of Physics, University of California, Berkeley, California 94720
and Materials Science Division, Lawrence Berkeley Laboratory, Berkeley, California 94720
(Received 17 December 1990; revised manuscript received 21 March 1991)

By using a model dielectric matrix in electron self-energy evaluations the computational effort of a quasiparticle band-structure calculation for a semiconductor is greatly reduced. Applications to various systems with or without inversion symmetry, having narrow or wide band gaps, and semiconductor alloys demonstrate the reliability and accuracy of the method. Calculations have been performed for thirteen semiconducting or insulating materials: Si, LiCl, AlP, AlAs, AlSb, GaP, GaAs, GaSb, InP, InAs, InSb, and the $Al_{0.5}Ga_{0.5}As$ and $In_{0.53}Ga_{0.47}As$ alloys. Excellent agreement with experimental results is obtained for the quasiparticle energies for these materials. The only three exceptions, $E(\Gamma_{1c})$ of AlP, $E(L_{1c})$ of AlAs, and $E(L_{1c})$ of AlSb are discussed and attributed to various experimental uncertainties. Several other quasiparticle-excitation-related properties are also examined in this work. The many-body corrections to the eigenvalues of the valence-band-maximum states obtained from the local-density approximation are calculated for the zinc-blende-structure semiconductors, which are widely used in semiconductor-interface studies. In the present approach, the static screening of the Coulomb interaction between two electrons in a crystal is determined using a model that depends only on the local charge densities at these two points. Since a direct quantitative modeling of the electron self-energy operator has proven difficult, the successful application of the present model-dielectric-function scheme in self-energy calculations makes possible detailed studies of the quasiparticle properties of rather complex systems, which would be otherwise computationally too demanding.

I. INTRODUCTION

Recently, much progress has been made in the band-structure calculations of solids from first principles.[1–13] By utilizing the many-body Green's-function technique, the quasiparticle energy calculations become conceptually well founded. Actually calculated results are, in general, in agreement with spectroscopic experiments to the order of 0.1 eV.[3] This general accordance has been established for semiconductor bulk systems,[6–8] as well as for their surfaces,[9,10] interfaces,[11] superlattices,[12] and also for some simple metals.[13] In contrast, the Hohenberg-Kohn-Sham local-density approximation (LDA) theory[14] for the inhomogeneous electron gas is very capable of describing the structural properties[15] but lacks rigorous justification when applied to excitation energies in a crystal.[15–17] However, it serves as a good starting point for the quasiparticle self-energy calculations.[3,6]

In the quasiparticle picture of electronic excitations in solids, the electron self-energy operator Σ is a central object.[1–3] It is, in general, nonlocal, non-Hermitian, and energy dependent with its imaginary part giving the lifetime effects. Currently, most quasiparticle calculations employ the so-called GW approximation of Hedin.[1,3–13] In this approximation, the vertex function is taken to be unity in the expression of Σ in terms of the dressed Green's function G and the dynamically screened Coulomb interaction W.[1] For semiconductors with significant charge nonuniformity, local field effects in the screening of the Coulomb interaction are shown to be of crucial importance in obtaining accurate energies at the 0.1-eV level.[3,6] Although they have been very successful in evaluating and predicting quasiparticle energies for various kinds of solid-state systems, these first-principles calculations are computationally time consuming. Several such calculations on semiconductor surfaces[9,10] and superlattices[12] approach the limit of current computational ability.

Owing mainly to the dependence in energy and the nonlocality in space of the self-energy operator Σ, to date, it has not been successful to introduce simplified and physically appealing models for Σ in real materials. The complexities of Σ also make it difficult to assess the correctness of the different aspects of a model should it fail to give results in agreement with experiments. It has been generally recognized[6] that the inclusions of the local fields in the screening and of the dynamical correlation effects are both crucial. The band gaps are usually only a small portion (10% or so) of the value of the electron self-energy, so a small error in modeling Σ can unfortunately introduce relatively much larger errors to the band gap or excitation energy results. Recently, several noteworthy attempts[5,18–20] have been made along this direction and some encouraging results are obtained. However, none of the simplified models for Σ have been fully successful even for the conventional semiconductors.[4,5,18–20] A particular difficulty is to calculate the indirect band gaps which require accurate treatment of the local fields.[6]

In this work, we take the alternative approach intro-

duced in Ref. 21: Instead of modeling Σ directly, we model the dielectric matrix, particularly the static dielectric matrix, which enters the evaluation of Σ. Its properties are rather well understood and relatively easier to handle. From a more technical point of view, calculation of the dielectric matrix takes about 75% or so of the total computation time for the crystalline semiconductors when a generalized plasmon-pole (GPP) model is used[6,8] in describing the energy dependence of the dynamical screening.

We have employed a generalized form of the static Levine-Louie model dielectric function[22] for semiconductors and insulators. This model incorporates the correct limiting cases of the long-range and short-range properties of the response function. It contains features of the response function resulting from the presence of a gap in the excitation spectrum.[22] Previous work[21] using this model dielectric matrix scheme has been reported for diamond, Si, and Ge. Here we generalize the approach to LiCl, AlP, AlAs, AlSb, GaP, GaAs, GaSb, InP, InAs, InSb, and $Al_{0.5}Ga_{0.5}As$ and $In_{0.53}Ga_{0.47}As$ alloys. These materials cover a range of semiconductor systems with quite different properties and chemical environments. The band gaps of them vary from 0.2 to 9.4 eV, for example.

For the materials studied, we have found excellent agreement between the calculated quasiparticle energies and the band structure obtained by various experiments. Table I summarizes this agreement for the minimum band gaps, in which we compare the LDA results, the first-principles quasiparticle calculation results where available, the present quasiparticle calculations with use of the model static dielectric function, and the experimental results. The first-principles results for InAs and InSb are calculated here using parameters similar to those in previous AlAs and GaAs calculations. The agreement between our model calculation and the experiment is generally within 0.1 eV. The largest discrepancies are less than 0.3 eV. Throughout the paper, the experimental results are taken from Ref. 23 except where specified. The agreement between the model and the full calculation is excellent (with maximum error less than 0.1 eV). Examining the small differences between them, there appears to be a systematic trend that the band gaps tend to be slightly overestimated for wide gap materials, and slightly underestimated for the narrow gap materials by the model. Table II gives our calculated quasiparticle valence-band widths for the thirteen materials, in comparison with existing experimental data. The agreement is again very good. For those materials for which there are no experimental valence-band widths, our results should provide a guide in analyzing x-ray and ultraviolet photoemission spectra.

In this work, a quasiparticle excitation-related parameter, the renormalization factor Z, is also examined and compared to the results from the first-principles calculations using the Hybertsen-Louie implementation of the GW approximation. Other GW calculations which do not employ the GPP model have given very similar results for Z.[7] Further, we study the many-body corrections to the LDA energies of the valence-band maxima (VBM) of the zinc-blende-structure semiconductors. The corrections are relevant to a quantitative theory of the valence-band offsets at semiconductor interfaces.

The remainder of this paper is organized as follows. Section II outlines the theoretical framework and gives the numerical details. In Sec. III we present the calculated quasiparticle energies for the thirteen materials and compare them with experiments. We also compare the quasiparticle energies from the present calculation with those from the full calculations where available. Section IV comprises discussions on several subjects, including some systematic trends of Σ, comparison of the static model dielectric function with the *ab initio* dielectric

TABLE I. The comparison of the LDA minimum band gaps, quasiparticle minimum band gaps from the available quasiparticle calculations (QP), and those from the present calculations with the model dielectric matrix (QPM), with experimental values taken from Ref. 23 except where noted. Results are in eV.

	LDA	QP	QPM	Expt.
Si	0.54	1.38	1.32	1.17
LiCl	6.07	9.21	9.34	9.40[a]
AlP	1.52		2.59	2.50
AlAs	1.25	2.06	2.15	2.23
AlSb	0.99		1.64	1.68
GaP	1.82		2.55	2.39
GaAs	0.37	1.29	1.22	1.52
GaSb	−0.10		0.62	0.80
InP	0.57		1.44	1.42
InAs	−0.39	0.40	0.31	0.41
InSb	−0.51	0.18	0.08	0.23
$Al_{0.5}Ga_{0.5}As$	1.12		2.06	2.09
$In_{0.53}Ga_{0.47}As$	0.02		0.80	0.81

[a]Reference 24.

TABLE II. Calculated quasiparticle valence-band widths for thirteen semiconductors and insulators in comparison with available experimental data taken from Ref. 23 except where noted. Results are in eV.

	Theory	Expt.
Si	12.30	12.5
LiCl	14.77	15.0[a]
AlP	12.07	
AlAs	12.41	
AlSb	11.10	
GaP	12.83	12.30
GaAs	13.03	13.21
GaSb	11.72	11.64
InP	11.75	11.0
InAs	12.10	12.30
InSb	10.91	11.7,[b]11.20[c]
$Al_{0.5}Ga_{0.5}As$	12.74	
$In_{0.53}Ga_{0.47}As$	12.46	

[a]Reference 25.
[b]Reference 26.
[c]Reference 27.

function, and examination of other quasiparticle excitation properties. Finally, a summary is given in Sec. V.

II. THEORY AND TECHNICAL DETAILS

In many-body Green's-function theory, the wave function and the eigenvalues of a quasiparticle in a crystal are given by solving the following Dyson equation:[1]

$$(T+V_{\rm ion}+V_h)\psi_{n,k}(\mathbf{r})+\int d^3\mathbf{r}'\Sigma(\mathbf{r},\mathbf{r}',E^{\rm qp}_{n,k})\psi_{n,k}(\mathbf{r}') = E^{\rm qp}_{n,k}\psi_{n,k}(\mathbf{r}) . \quad (1)$$

The terms in Eq. (1) represent, respectively, the kinetic energy, the ionic potential, the Hartree average potential, and the electron self-energy operator Σ which contains the electron-electron exchange and correlation effects. In the GW approximation,[1] Σ becomes

$$\Sigma(\mathbf{r},\mathbf{r}';E)=\frac{i}{2\pi}\int d\omega\, e^{-i\delta\omega}G(\mathbf{r},\mathbf{r}';E-\omega)W(\mathbf{r},\mathbf{r}';\omega) , \quad (2)$$

where G is the dressed Green's function, W is the dynamically screened Coulomb interaction, and δ is a positive infinitesimal. More details of the theory can be found in the articles by Hedin and by Hedin and Lundqvist.[1] The formalism and calculational scheme for semiconductors and insulators and the effects of many-electron screening have been extensively discussed by Hybertsen and Louie.[3,6]

In the Hybertsen-Louie scheme[6,8] which is employed in this work, the calculation of the electron self-energy is formulated in momentum space. In first-principles calculations, the static irreducible polarizability matrix χ_0 is evaluated as a ground-state property from the LDA results using the Adler-Wiser[28] perturbative approach. This part of the calculation involves summations over large numbers of intermediate states for each element of the χ_0 matrix. It typically takes 75% or so of the total computation time. The random-phase approximation (RPA) is then used to calculate $\epsilon^{-1}(\omega=0)$ from χ_0.[3,6] In the present work, a generalized Levine-Louie model[22] which we will discuss later is used for the static dielectric matrix. The static dielectric function is as in the full calculation extended to finite frequencies by the generalized plasmon-pole (GPP) model.[6,8] Exact sum rules are used to fix the locations and the strengths of the plasmon poles in $\epsilon^{-1}(\omega)$.[6,8] For systems without inversion symmetry, special care needs to be taken for the phase factors in applying the GPP model.[8] The integral over frequency in Eq. (2) can be easily carried out analytically. The time-ordered Green's function is constructed iteratively within the quasiparticle approximation and, for the first run, its LDA counterpart is used. Once both G and W ($W=\epsilon^{-1}V$ with V the bare Coulomb interaction) are obtained, the quasiparticle energies are calculated as

$$E^{\rm qp}_{n,k}=\epsilon^{\rm LDA}_{n,k}+\langle n,\mathbf{k}|\Sigma-V^{\rm xc}_{\rm LDA}|n,\mathbf{k}\rangle , \quad (3)$$

where $V^{\rm xc}_{\rm LDA}$ is the LDA exchange-correlation potential. The last term in Eq. (3) is often referred to as the many-body correction to the LDA eigenvalue of the state $|n,\mathbf{k}\rangle$. The validity of Eq. (3) is based on the observation that the quasiparticle wave functions are very well approximated by the LDA wave functions.[6,7] The spectrum in the Green's function is subsequently updated to the quasiparticle energies after the first run. This self-consistency procedure increases the quasiparticle band gaps by roughly 0.1 eV except for LiCl in which case a 0.3-eV gain is found. More elaborate numerical integration[7] over frequency for Eq. (2) has yielded virtually identical results for the quasiparticle energies.

The rest of this section is devoted to a discussion of the form of a generalized Levine-Louie model dielectric matrix and the computational details of using it in quasiparticle self-energy calculations

A. Model dielectric matrix

Solving for the dynamical response function of a many-body system has been a very active and interesting area in the field of many-body physics.[29] A large number of physical quantities (pair distribution function, correlation energy, etc.) of a many-electron system can be calculated with a knowledge of the dielectric function $\epsilon^{-1}(\mathbf{q},\mathbf{q}';\omega)$. Since the early work of the Lindhard dielectric function,[30] attempts[29,31,32] have been made to go beyond the random-phase approximation, viz., to include the effects of the electron-electron exchange and correlation in the screening. A typical example of the theories along this line is the Hubbard model[31] which includes the exchange interaction within the context of the time-dependent Hartree-Fock theory.

The Levine-Louie model,[22] however, is not directly derived from a microscopic theory. Rather, it starts from realizing the presence of an energy gap in the electronic excitation spectrum in a semiconductor. The imaginary part of the dielectric function is chosen to be Lindhard-like with a reduced, "effective" frequency. Specifically, it is taken to be zero up to a frequency threshold determined by the gap. Defining

$$\lambda^2(r_s)=\frac{\omega_p^2(r_s(\mathbf{r}))}{\omega_F^2(r_s(\mathbf{r}))(\epsilon_0-1)}$$

and

$$\omega_-^2=\omega^2-(\lambda\omega_F)^2 ,$$

the imaginary part of the dielectric function is then expressed as

$$\mathrm{Im}\epsilon(q,\omega)=\begin{cases}\mathrm{Im}\epsilon^L(q,\omega_-), & |\omega|\geq\lambda\omega_F\\ 0, & |\omega|<\lambda\omega_F.\end{cases} \quad (4)$$

In Eq. (4), $\epsilon^L(q,\omega)$ represents the usual Lindard dielectric function.[22,30] Notice that the parameter λ is a function of the local charge density (which determines the local electron density parameter r_s) and of ϵ_0. The dielectric constant ϵ_i (ϵ_∞ for ionic crystals) is the input needed for the

model. The real part is then obtained from Kramers-Kronig causality requirements. In the absence of the gap, the model reduces exactly to the RPA Lindhard dielectric function. This model generally agrees well with other model dielectric functions, and for the case of Si, it compares better[22] with the realistic calculation by Walter and Cohen.[33] The expression for the static dielectric function from this model is given by (in atomic units)

$$\epsilon_{\mathrm{LL}}(\mathbf{r},q)=1+\frac{2}{\pi q_F}\left[\frac{1}{Q^2}-\frac{\lambda}{2Q^3}\left[\tan^{-1}\frac{2Q+Q^2}{\lambda}+\tan^{-1}\frac{2Q-Q^2}{\lambda}\right]+\left[\frac{\lambda^2}{8Q^5}+\frac{1}{2Q^3}-\frac{1}{8Q}\right]\ln\left[\frac{\lambda^2+(2Q+Q^2)^2}{\lambda^2+(2Q-Q^2)^2}\right]\right], \tag{5}$$

with $Q=q/q_F(r_s)$.

In the original work by Levine and Louie,[22] the parameters q_F and λ are taken to be the average values characteristic of the specific material. The model dielectric function in this form (that of a *homogeneous insulating* electron gas) has been employed by Wang and Pickett in their quasiparticle LDA theory.[5] Here, as in Ref. 21, it is used to model the static screening potential between $\mathbf{r}$ and $\mathbf{r}'$ in the following way:

$$V^{\mathrm{scr}}(\mathbf{r},\mathbf{r}')=\tfrac{1}{2}[V^{\mathrm{scr}}_{\mathrm{LL}}(\mathbf{r}-\mathbf{r}';r_s(\mathbf{r}'))+V^{\mathrm{scr}}_{\mathrm{LL}}(\mathbf{r}'-\mathbf{r};r_s(\mathbf{r}))]\ . \tag{6}$$

Both terms are evaluated using Eq. (5). By using the local values for the parameters in the model, we obtain a better description of the screening in the *inhomogeneous insulating* electron gas in a semiconductor. This generalization also ensures the proper symmetry under the interchange of $\mathbf{r}$ and $\mathbf{r}'$ in $V_{\mathrm{scr}}(\mathbf{r},\mathbf{r}')$. We emphasize that our model screening function is only for the static response. The dynamical effects will certainly change this screening picture, as accounted for by the GPP model in the Hybertsen-Louie scheme.[6,8]

A straightforward manipulation of Eq. (6) gives the following form of the static dielectric matrix in momentum space:[21]

$$\epsilon^{-1}_{GG'}(\mathbf{q};\omega=0)V_c(\mathbf{q}+\mathbf{G}')=\frac{1}{2}\left[V_c(\mathbf{q}+\mathbf{G})\int d\mathbf{r}'\epsilon^{-1}_{\mathrm{LL}}[|\mathbf{q}+\mathbf{G}|;r_s(\mathbf{r}')]e^{i(\mathbf{G}'-\mathbf{G})\cdot\mathbf{r}'}+V_c(\mathbf{q}+\mathbf{G}')\int d\mathbf{r}\,\epsilon^{-1}_{\mathrm{LL}}[|\mathbf{q}+\mathbf{G}'|;r_s(\mathbf{r})]e^{i(\mathbf{G}'-\mathbf{G})\cdot\mathbf{r}}\right]. \tag{7}$$

The model requires only one parameter as input, namely, the dielectric constant of the material. It can in principle be evaluated from *ab initio* calculations,[34] but in this work, the experimental values are used. The final quasiparticle energies are not very sensitive to the exact value of ϵ_0 because short-range screening is not strongly affected by ϵ_0. For silicon, for example,[21] the band gaps change by less than 0.1 eV in a range of variation of 10% or so of ϵ_0. We stress that both the short-range metallic screening behavior and the long-range semiconducting screening are properly retained by the model.

B. Technical details

Table III gives the lattice constants and the dielectric constants for Si, LiCl, AlP, AlAs, AlSb, GaP, GaAs, GaSb, InP, InAs, and InSb, as well as for $Al_{0.5}Ga_{0.5}As$ and $In_{0.53}Ga_{0.47}As$, used in our calculation. For ionic crystals, it is understood that we mean ϵ_∞ when we mention the dielectric constants. These constants are taken from Ref. 23. We have also included the energy cutoffs for the expansion of the wave functions in the LDA calculations for these materials in Table III (see below). For the two semiconductor alloys, the lattice constants and the dielectric constants are taken to be the weighted arithmetical averages of the constituent III-V compounds. ($In_{0.53}Ga_{0.47}As$ is lattice matched with InP.)

In the calculations, *ab initio* pseudopotentials[35] are used to eliminate core electrons, and to remove the strong Coulomb potential in the core region responsible for binding them, from the problem. Scalar relativistic

TABLE III. Lattice constants (in Å) and static dielectric constants (ϵ_∞ for ionic crystals) taken from Ref. 23, and the energy cutoffs (in Ry) for the wave functions used in the calculation.

	a_0	ϵ_∞	E_{cut}
Si	5.43	12.0	16
LiCl	5.13	2.7	25
AlP	5.45	7.5	16
AlAs	5.65	8.2	16
AlSb	6.14	10.0	14
GaP	5.45	9.0	16
GaAs	5.65	10.9	16
GaSb	6.10	14.4	14
InP	5.87	9.6	14
InAs	6.04	12.3	14
InSb	6.47	15.7	13
$Al_{0.5}Ga_{0.5}As$	5.65	9.5	16
$In_{0.53}Ga_{0.47}As$	5.87	11.6	14

effects are included except for Si and LiCl. The Ceperley-Alder exchange-correlation potential[36] is used in the LDA calculations. However, in examining the absolute many-body corrections to the LDA energies at the top of the valence band, the von Barth–Hedin form[37] of the exchange-correlation potential is employed. It is more appropriate in this case since the von Barth–Hedin approximation to the exchange-correlation potential in the LDA corresponds to the GW approximation in jellium. The calculation of the self-energy operator Σ involves several numerical cutoffs. For GaAs, the LDA wave functions are expanded up to $E_{\max}=16$ Ry. The LDA band gaps are converged to better than 0.01 eV. The dielectric matrix is truncated at $|\mathbf{q}+\mathbf{G}|=3.1$ in Ry atomic units. We have included 8 $\mathbf{k}$ points in the irreducible wedge of the Brillouin zone and 100 bands in the calculation of the matrix elements of Σ in summing over the immediate scattering states. The final quasiparticle energies are converged to about 0.1 eV. Similar convergence is reached for all the other materials with the energy cutoffs given in Table III. Among them, LiCl has the largest cutoffs. Two partially canceling effects, the core relaxation and the valence-core exchange, are taken into account within the LDA by the LDA atomic pseudopotentials.[6,7]

For some systems, the LDA minimum band gaps are negative. But the occupation number in the Green's function should be determined by the quasiparticle spectrum. This is achieved self-consistently. We first input the LDA spectrum into the Green's function. The occupation of these states is then adjusted according to the new quasiparticle spectrum for the second run. This procedure distinguishes better the valence states from the conduction states, and yields a larger band gap mainly due to changes in the exchange energies associated with the states.

The virtual crystal approximation[38] (VCA) has been employed in calculating the properties of $Al_{0.5}Ga_{0.5}As$ and $In_{0.53}Ga_{0.47}As$. The ionic pseudopotential of the virtual cation is obtained by the direct weighted average of the pseudopotentials of the two constituent cations. The electron-electron interaction potential is allowed to adjust self-consistently to the charge density distribution in the virtual crystal, given the virtual ionic pseudopotentials. No attempts are made to include chemical disorder[39] and/or bond-length disorder.[40] The roles of these disorders have yet to be clarified by careful comparisons between experimental results and theoretical predictions.[41]

The effects of spin-orbit interactions become nonnegligible for materials which contain heavier atoms.[42,43] In Sb-containing zinc-blende-structure compounds, the spin-orbit splitting at the top of valence band can be as large as 0.7–0.8 eV. This alters the direct gap at Γ in InSb by more than 50%. We have taken the experimental spin-orbit splitting parameters where they are available. *Ab initio* calculations for the spin-orbit interaction effects in the diamond- and zinc-blende-structure semiconductor compounds[42,43] have been carried out. The results give accurate accounts for the spin-orbit interaction induced band splittings.[42,32] Spin-orbit effects arise from the electron-ion interaction. They can be well treated to first order in perturbation within the LDA and would not affect the many-electron contribution to the quasiparticle results.[42,43]

III. QUASIPARTICLE ENERGIES FOR THIRTEEN SEMICONDUCTORS

In this section we present our theoretical quasiparticle energies for the thirteen materials, together with the available experimental results. For completeness, we have also included Si although it was discussed previously in Ref. 21. The results (both *ab initio* and model dielectric function calculations) reported here for silicon are newly calculated with parameters similar to those used for the other compounds to facilitate comparison. First-principles quasiparticle energies without using the model dielectric function for InAs are calculated here for the first time. As evidenced by the satisfactory agreement for all the materials investigated, the model demonstrates clearly its versatility and accuracy in the quasiparticle self-energy calculations for semiconductors and insulators. We report our results for Si and LiCl, both having inversion symmetry, in Sec. III A. The results for the nine zinc-blende-structure semiconductor compounds are given in Sec. III B. Section III C contains the results for the two semiconductor alloys.

Before we proceed to the comparison of the theory with the experiment, we would like to note that the interpretation of our calculated results is based upon a quasiparticle description of excitations in solids. The evaluated poles in the one-particle Green's function represent the energies of the excitations in which one particle is physical removed from or added into the system. Hence strictly speaking, *direct* comparison can only be made to photoemission and inverse photoemission experiments. Band gaps and critical transition energies derived from differences in quasiparticle energies may differ from results obtained from optical measurements in which electron-hole pairs are created. In general, excitonic effects shift the optical transition energies to lower values by the amount of the exciton binding energy if bound excitons are formed and may modify the shape of optical spectrum. In three dimensions, the change in excitation energy caused by excitons is less than 0.05 eV at interband critical points in most semiconductors. Our following comparison with experimental data proceeds on the assumption that excitonic effects are small in these materials compared to the energies of interests.

A. Si and LiCl

Si is one of the most carefully studied semiconductors. It is in the diamond structure under normal pressure with an indirect band gap 1.17 eV ($\Gamma_{25v}\rightarrow\sim 0.85X_{1c}$). LiCl is a wide gap insulator (with a band gap $\Gamma_{15v}\rightarrow\Gamma_{1c}\sim 9.4$ eV) in the NaCl structure. The screening effects in LiCl are much weaker than those in Si, as manifested by their respective dielectric constants: 2.7 for LiCl and 12 for Si. The quasiparticle wave functions (as well as the charge density) are so localized in LiCl that it poses a special challenge to the model-dielectric-function scheme since

the model owes its origin to the isotropic and homogeneous electron gas. Despite these concerns, we find that the model calculation gives 9.34 eV for the minimum gap for LiCl, in excellent agreement with 9.4 eV deduced from reflectivity measurement.[24] The minimum gap from our model calculation is slightly larger than the full calculation result 9.21 eV, consistent with a trend that we mentioned earlier.

Tables IV and V show the excellent agreement for both of these materials between the quasiparticle energies obtained with use of the model dielectric function and the results from first-principles calculations. Spin-orbit interactions change the band gaps by less than 0.05 eV in these two materials and are therefore neglected. The very minor differences of the first-principles quasiparticle energies of Si and LiCl here and those reported in Ref. 6 are due to a slightly lesser convergence in the present calculation. For Si, we have included the available experimental results taken from Ref. 6. For LiCl, we only make the comparison between the LDA eigenvalues, the quasiparticle energies from the model and the full calculations due to a lack of reliable experimental data. The point here for LiCl is to illustrate the applicability of the model dielectric matrix in the self-energy calculation for extremely ionic insulators. The success hinges on the fact that the model dielectric function takes into account the rather drastic variation of the charge accumulation in LiCl.

The largest discrepancy between the model and the full calculation in LiCl occurs for the Cl 3*s*-like states. We find this is due to the less efficient screening of the model. This affects the self-energies of the Cl 3*s*-like states the most since it has the largest (absolute) value of Σ. This less efficient screening pushes the energies of the 3*s*-like states further down (thus closer to the Hartree-Fock result), hence a larger valence-band width. The larger band gap found in the model calculation also stems from the same origin.

TABLE IV. Comparison of the quasiparticle energies from the present model calculation (QPM) and from the full first-principles calculation (QPF) with experimental values for Si taken from Refs. 6 and 23 at high-symmetry **k** points. Energies are in eV.

	QPM	QPF	Expt.
Γ_{1v}	−12.30	−11.98	−12.5[a]
Γ'_{25v}	0.0	0.0	0.0
Γ_{15c}	3.43	3.43	3.4[b]
Γ'_{2c}	4.23	4.13	4.2[a]
X_{1v}	−8.15	−7.97	
X_{4v}	−3.02	−2.95	−2.9,[b] −3.3[b]
X_{1c}	1.47	1.53	
L'_{2v}	−9.98	−9.74	−9.3[a]
L_{1v}	−7.28	−7.12	−6.7[a]
L'_{3v}	−1.28	−1.25	−1.2[a]
L_{1c}	2.36	2.34	2.1,[b] 2.4[b]
L_{3c}	4.30	4.30	4.15[b]

[a]Reference 23.
[b]Reference 6 and references therein.

TABLE V. Comparison of the LDA eigenvalues, the quasiparticle energies calculated from the model (QPM), and the quasiparticle energies from the full calculations (QPF) for the ionic crystal LiCl. Energies are in eV.

	LDA	QPM	QPF
Γ_{1v}	−13.11	−14.77	−13.33
Γ_{15v}	0.0	0.0	0.0
Γ_{1c}	6.07	9.34	9.21
Γ'_{25c}	11.84	15.71	15.63
X'_{1v}	−11.95	−13.64	−12.30
X'_{4v}	−2.40	−2.74	−2.68
X'_{5v}	−1.00	−1.14	−1.11
X_{1c}	7.87	11.16	11.18
X_{3c}	8.45	11.94	11.95
L'_{1v}	−11.85	−13.61	−12.26
L'_{2v}	−2.58	−2.93	−2.87
L'_{3v}	−0.03	−0.08	−0.08
L_{1c}	6.38	9.82	9.78
L_{3c}	9.11	12.82	12.80

To gain some quantitative feel of the importance of the dynamical screening on the quasiparticle energies in alkali halides, we have broken Σ into two pieces in LiCl: the bare exchange and the rest of Σ which includes the screening to the bare exchange and the correlation terms. The bare exchange term gives essentially the Hartree-Fock results, which are of course identical in both the model and the *ab initio* calculations. In Table VI we list these terms for the top of the valence band Γ_{15v} and for the bottom of the conduction band Γ_{1c} from both the model and the full calculations. For the occupied state Γ_{15v}, which is largely of atomic Cl 3*p* character, the bare exchange contributes more than 85% to Σ. But for the unoccupied state Γ_{1c}, its contribution is only 50%. These numbers are not very different from those typical of a semiconductor.

B. Zinc-blende-structure compounds

In this subsection we shall discuss the quasiparticle energies for the nine zinc-blende-structure compounds formed by the combinations of Al, Ga, In with P, As, Sb. The empirical pseudopotential method has been successfully applied to these zinc-blende-structure materials.[44,45] It is, however, an empirical approach and thus requires experimental data as input. We show here that the present quasiparticle approach gives equally accurate excitation energies without fitting to experimental optical and photoemission spectra.

In Tables VII, VIII, and IX, we compare the calculated quasiparticle energies with the available experimental data, for compounds containing P, As, and Sb, respectively. Quasiparticle energies at Γ, X, and L are given in these tables. Spin-orbit interaction corrections are taken from experiments where available. They are most significant at Γ. For the P-containing compounds, the

TABLE VI. Comparison for the various terms in Σ at Γ in LiCl calculated using the model and using the *ab initio* static dielectric function. X denotes the bare exchange; SX+CH denotes the rest of Σ. Results are in eV.

	Full			Model		
	X	SX+CH	Σ	X	SX+CH	Σ
Γ_{15v}	−18.39	1.76	−16.64	−18.39	1.88	−16.51
Γ_{1c}	−4.26	−3.75	−8.01	−4.26	−3.50	−7.76

TABLE VII. Quasiparticle energies for AlP, GaP, and InP from present calculation compared to available experimental results taken from Ref. 23 except where noted. The results are in eV.

	AlP		GaP		InP	
	Theory	Expt.	Theory	Expt.	Theory	Expt.
Γ_{1v}	−12.07		−12.83	−12.30	−11.75	−11.0
Γ_{15v}	0.0	0.0	0.0	0.0	0.0, −0.11	0.0, −0.11
Γ_{1c}	4.38	3.62[a]	2.85	2.89	1.44	1.42
Γ_{15c}	5.72		5.03	4.87	5.08	4.85
X_{1v}	−9.68		−10.02	−9.6	−9.53	
X_{3v}	−5.69		−7.04	−6.8	−5.97	−5.9
X_{5v}	−2.31		−2.78	−3.0	−2.38	−2.2
X_{1c}	2.59	2.50	2.55	2.39	2.58	2.38
X_{3c}	3.56		2.81	2.75	3.08	
L_{1v}	−10.36		−10.91	−10.8	−10.18	
L_{1v}	−5.92		−6.88	−6.8	−5.89	
L_{3v}	−0.85		−1.16	−1.27	−1.02	−1.15
L_{1c}	3.90		2.67	2.64	2.28	2.03
L_{3c}	6.05		5.87		5.83	

[a]Reference 46.

TABLE VIII. Quasiparticle energies for AlAs, GaAs, and InAs from the present calculation compared to available experimental results taken from Ref. 23 except where noted. Energies are in eV.

	AlAs		GaAs		InAs	
	Theory	Expt.	Theory	Expt.	Theory	Expt.
Γ_{1v}	−12.41		−13.03	−13.21	−12.10	−12.30
Γ_{15v}	0, −0.27	0, −0.27	0, −0.34	0, −0.34	0, −0.38	0, −0.38
Γ_{1c}	2.88	3.13	1.22	1.52	0.31	0.41
Γ_{15c}	5.14		4.48	4.61	4.51	
X_{1v}	−10.41		−10.69	−10.86	−10.23	−9.8
X_{3v}	−5.87		−7.19	−6.81	−6.18	−6.30
X_{5v}	−2.44	−2.41	−2.87	−2.91	−2.49	−2.40
X_{1c}	2.14	2.23	2.01	1.90	2.01	
X_{3c}	3.03		2.24	2.47	2.50	
L_{1v}	−10.97		−11.41	−11.35	−10.76	−10.6
L_{1v}	−6.01		−6.97	−6.81	−6.04	
L_{3v}	$E_{L_{1c}}$ − 3.90	$E_{L_{1c}}$ − 3.92	−1.28	−1.41	−1.13	−1.04
L_{1c}	2.91	2.36[a]	1.64	1.74	1.43	1.55
L_{3c}	5.59		5.40		5.32	

[a]Reference 47.

TABLE IX. Quasiparticle energies for AlSb, GaSb, and InSb from the present calculation compared to available experimental results taken from Ref. 23 except where noted. Energies are in eV.

	AlSb		GaSb		InSb	
	Theory	Expt.	Theory	Expt.	Theory	Expt.
Γ_{1v}	−11.10		−11.72	−11.64	−10.91	−11.7,[a] −11.2[b]
Γ_{15v}	0, −0.67	0, −0.67	0, −0.76	0, −0.76	0, −0.80	0, −0.80
Γ_{1c}	2.23	2.32	0.62	0.82	0.08	0.23
Γ_{15c}	3.52,3.82	3.7,4.0	3.11,3.32	3.2,3.4	3.16,3.55	3.14,3.53
X_{1v}	−9.09		−9.33	−9.62	−9.00	−9.50[a]
X_{3v}	−6.01		−7.26	−6.90	−6.33	−6.40
X_{5v}	−2.54		−2.73, −2.97	−2.86, −3.10	−2.56	−2.40
X_{1c}	1.64	1.68	1.15	1.15	1.50	1.79
X_{3c}	1.84		1.50		1.57	
L_{1v}	−9.70		−10.16	−10.06	−9.61	−10.5[a]
L_{1v}	−5.91		−6.78	−6.60	−5.97	
L_{3v}	$E_{L_{1c}}$ −3.32	$E_{L_{1c}}$ −3.31	−1.56, −1.14	−1.53, −1.10	−1.46, −0.96	−1.4, −0.9
	$E_{L_{1c}}$ −2.90	$E_{L_{1c}}$ −2.89				
L_{1c}	1.84	2.33[c]	0.79	0.92	0.76	
L_{3c}	4.29		4.11,4.23	4.36,4.49	4.09,4.24	4.32,4.47

[a]Reference 26.
[b]Reference 27.
[c]Reference 48.

spin-orbit splittings (<0.1 eV) are neglected. For As-containing compounds, we only consider the spin-orbit correction to the valence-band maximum (splitting of ~ 0.3 eV). For Sb-containing compounds, they should be included for all the **k** points and we have taken the available experimental data for the energy splitting caused by spin-orbit interaction (0.4–0.8 eV depending on **k**). Simple group notation is used throughout the paper. Wherever two energies are listed in the same entry, they represent the energies of two states (at Γ, one of them could still be doubly degenerate) derived from the originally degenerate states. Later in the paper, we will discuss some systematic trends in the quasiparticle energies in these compounds.

The experimental data are taken from Ref. 23. The original sources of the data scatter in the literature, with rather diverse origin. We only include references of the experimental data which we will discuss further below. The overall agreement between theory and experiment is excellent. Here we analyze only the three near gap states with energies that show discrepancies larger than 0.25 eV. They all occur in the Al-containing compounds. For AlP, the theory gives a direct gap at Γ of 4.38 eV, while the experimental value is 3.62 eV.[46] For AlAs, the theory and experiments agree on the direct gap at L, which is 3.90 eV from theory and 3.92 eV from experiment.[23] But the indirect gap in AlAs from Γ_{15v} to L_{1c} are 2.91 eV from the theory and 2.36 eV from experiment,[47] showing a 0.55-eV difference. The energy of the L_{1c} state in AlSb given by theory is 1.84 eV above the valence-band maximum, but the experimental value is 2.33 eV,[48] although again, there is a very good agreement for the direct transition energies at L. All of these three discrepancies exceed 0.5 eV and are not expected to be caused by the uncertainties in the calculation. Simple estimates of the exciton energies from the experimental effective masses and dielectric constants in these compounds cannot account for more than 0.03 eV. For these three materials (as well as the other six materials), the rest of the quasiparticle energies consistently agree very well with experiments. This leads us to reexamine the experimental data.

The experimental value for the direct band gap of AlP is obtained from photoluminescence spectrum by Monemar.[46] Due to a large defect concentration in the AlP sample used, the observed spectrum is rather broad and the features are rather vague, compared to those of AlAs reported in the same paper. The temperature dependence of this gap was not studied due to the large uncertainty in locating the transitions. There is effectively little evidence for the weak feature observed to be a direct band gap. The feature at 3.62 eV, assumed to be the direct-band-gap energy at Γ in the experiment, actually agrees with our theoretical energy of X_{3c}, which is 3.56 eV. The transition to X_{3c} from Γ_{15v} involving a phonon or defect potential is possible. We thus believe the experimental data are not conclusive in the identification of the direct band gap in AlP.

The inconsistency between theory and experiment for the position of L_{1c} relative to Γ_{15c} in AlAs was also reported in a paper by Godby, Schlüter, and Sham,[7] in which first-principles GW calculation was performed. Our calculated result of 2.91 eV agrees with their value of 3.03 eV for the energy of L_{1c}. It was pointed out in their analysis[7] that the experimental energy of L_{1c} was not directly measured, but was extrapolated quadratically from the data of $Al_xGa_{1-x}As$ alloys.[47] However, the ex-

TABLE X. Comparison of the full quasiparticle calculation with results from the model dielectric matrix calculation for AlAs, GaAs, and InAs. Results presented are the many-body corrections defined in Eq. (3) for states near the gap. Results are in eV.

	AlAs		GaAs		InAs	
	Full	Model	Full	Model	Full	Model
Γ_{15v}	0.00	0.00	0.00	0.00	0.00	0.00
Γ_{1c}	0.92	1.03	0.91	0.84	0.79	0.70
X_{5v}	−0.14	−0.16	−0.08	−0.12	−0.03	−0.06
X_{1c}	0.80	0.87	0.73	0.70	0.71	0.61
L_{3v}	−0.07	−0.08	−0.03	−0.05	−0.01	−0.02
L_{1c}	0.84	0.94	0.81	0.77	0.77	0.67

perimental range of x only goes from 0.0 to 0.6.[47] The discrepancy was attributed to the inaccuracy of the quadratic fit used in analyzing the experimental data.

There are early experiments on the energy position of L_{1c} in AlSb by Mead and Spitzer,[49] which gives 1.86 eV in very good agreement with our theory. Photoresponse was measured and this energy was deduced from the slope of the photoresponse. In Ref. 48, very accurate modulation reflectance technique was used. But there does not appear to be sufficient evidence for associating the peak in the modulation reflectance spectrum with the energy of L_{1c}, although the positions of the peaks can be accurately located. The peak attributed to L_{1c} in this paper did not appear in the low-field electroreflectance spectra. Similar features in the electroreflectance spectra are observed in GaAs, where they are attributed to possible defect states. In Ref. 48, measurement had not been done at energies below 2.0 eV to observe the L_{1c} peak predicted by the present calculation. So our theoretical result is not incompatible with this high-accuracy electroreflectance experiment. Further experiments are needed to elucidate these disagreements.

First-principles quasiparticle energies are available for AlAs for GaAs (Refs. 7 and 8) and we have performed similar calculation for InAs. In Table X we display the excellent comparison of the many-body corrections to the LDA eigenvalues of the band edge states at Γ, X, and L between results from the model calculation with those obtained from first principles. We find as in Ref. 21 that the model gives values for Σ for these states to within 5% of the first-principles results. The difference in the corrections to the LDA results for the direct band gaps are even smaller between the model and the full calculations. They are for most cases less than 1%. From Table X and results on other semiconductors, we observe that empirically when the minimum gap in a semiconductor is larger than 1.5 eV, the model calculation gives slightly larger band gaps than the full calculation. When the minimum gap is smaller than 1.5 eV, the model results are smaller. But the differences in the quasiparticle energies between the model and the full calculations are consistently within 0.1 eV.

C. Semiconductor alloys

Semiconductor alloys have attracted much attention because of their tunable band gaps and other tunable properties. Among them, $Al_{0.5}Ga_{0.5}As$ and $In_{0.53}Ga_{0.47}As$ are probably the most studied and best known ones. The latter has a potential of being useful in fast electronic devices. Several theoretical methods[38–41] have been employed in the past for calculating semiconductor alloy electronic properties. The virtual crystal approximation[38] (VCA) which omits local chemical and bond-length fluctuations is the simplest and has been the most popular approach. More sophisticated theories[39,40] have recently been proposed and they reveal certain deficiencies of the VCA method. But, as far as the absolute band structure is concerned (rather than the much smaller differences between the band gap of the alloy and the averaged value of the corresponding band gaps of the constituent semiconductors), calculations have shown that VCA and other more sophisticated methods give the same results to within 0.1 eV.[39,40] We find that the bowing parameters of the band gaps are not given correctly by either LDA or the present quasiparticle approach *within the* VCA. The roles of chemical disorder and bond-length disorder in determining the bowing parameters are qualitatively important but the details have yet to

TABLE XI. Quasiparticle energies for $Al_{0.5}Ga_{0.5}As$ and $In_{0.53}Ga_{0.47}As$ from the present calculation, in comparison with experiments. Energies are in eV.

	$Al_{0.5}Ga_{0.5}As$		$In_{0.53}Ga_{0.47}As$	
	Theory	Expt.	Theory	Expt.
Γ_{1v}	−12.74		−12.46	
Γ_{15v}	0, −0.30	0, −0.30	0, −0.30,	0, −0.30
Γ_{1c}	2.06	2.09[a]	0.80	0.81[b]
Γ_{15c}	4.77		4.55	
X_{1v}	−10.57		−10.42	
X_{3v}	−6.54		−6.49	
X_{5v}	−2.68		−2.64	
X_{1c}	2.05	1.97[a]	2.07	
X_{3c}	2.61		2.50	
L_{1v}	−11.21		−11.02	
L_{1v}	−6.51		−6.36	
L_{3v}	−1.16		−1.18	
L_{1c}	2.25	2.03[a]	1.63	
L_{3c}	5.48		5.41	

[a]Reference 47.
[b]Reference 50.

be clarified.[41]

In Table XI the quasiparticle energies at Γ, X, and L are given for the two semiconductor alloys considered, in comparison to the available experimental data. For $Al_{0.5}Ga_{0.5}As$, the theory places $E(L_{1c})$ at about 0.2 eV higher than $E(\Gamma_{1c})$, and $E(X_{1c})$. This concentration is in the vicinity of that of the Γ_{1c}, X_{1c}, and L_{1c} crossovers. Experimentally the energies of these **k** points are very close to each other. Among them, X_{1c} is identified as the conduction-band minimum. We note $E(\Gamma_{1c})$ from the theory is a little too low for both parent compounds, AlAs and GaAs, due to the neglect of core-valence exchange interaction.[6,7] Taking this into account in our calculation would raise $E(\Gamma_{1c})$ to approximately $E(L_{1c})$, leaving unambiguously X_{1c} the conduction-band minimum. For $In_{0.53}Ga_{0.47}As$ experimental data are not complete in terms of the band energies. The use of the VCA also prohibits a reliable estimate for the band bowing parameters in these semiconductor alloys. No systematic agreement with experiments is found for the bowing parameters in the analysis of our theoretical energies.

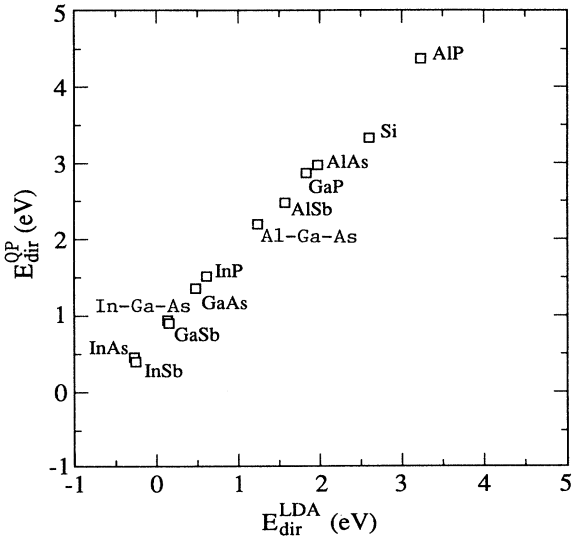

FIG. 1. The quasiparticle direct band gaps vs the LDA direct band gaps for Si, nine zinc-blende-structure compounds, and two semiconductor alloys.

IV. ANALYSIS AND DISCUSSIONS

We discuss some systematic trends found in the calculated quasiparticle energies and the electron self-energy operator in these semiconductor compounds in Sec. IV A. In Sec. IV B, the model static dielectric matrices are quantitatively compared to the first-principles dielectric matrices in several cases. The objective of Sec. IV C is to examine the quasiparticle renormalization factor which is related to the validity of the quasiparticle description of excitations in solids. In Sec. IV D, our results for the many-body corrections to the LDA energies at the valence-band maxima for the zinc-blende-structure semiconductors are reported.

A. Systematic trends in Σ

The complexities of Σ are caused by its nonlocality and its energy dependence. In the GW theory, they arise from both the Green's function G and the screened Coulomb interaction W. Their effects on the quasiparticle band gaps are found to cancel to some degree but quantitatively reliable results can only be acquired by including both. In Si, for example, the indirect minimum band gap requires definitely the inclusion of the local fields in W while the direct band gaps rely less on it.[6] The nine III-V compounds considered here provide an excellent family of semiconductor systems for us to study the systematic trends in the behavior of Σ.

For simplicity, we shall mainly discuss the direct band gaps at Γ of these compounds. The minimum band gaps are derived from different **k** points in the Brillouin zone, thus bringing unwelcome complications to the analysis. In all of these materials, the top of the valence band at Γ has characters of the bonding p states and they are all threefold degenerate without spin-orbit interaction. The lowest conduction-band state at Γ is formed by the antibonding s states for all the materials except for Si, in which it is formed by the antibonding p states. We plot, in Fig. 1, the quasiparticle band gaps versus the LDA band gaps for these compounds. Figure 2 depicts the variation of the many-body corrections to the LDA direct band gaps as the degree of localization of the states varies, being measured here by the ratio of the direct band gap at Γ and the valence-band width, as calculated by the theory. There is a general correlation between the many-body correction and the degree of wave-function localization in these materials. In Fig. 2, the data point for Si drops somewhat below the line that the other materials seem to follow. The origin of this difference stems

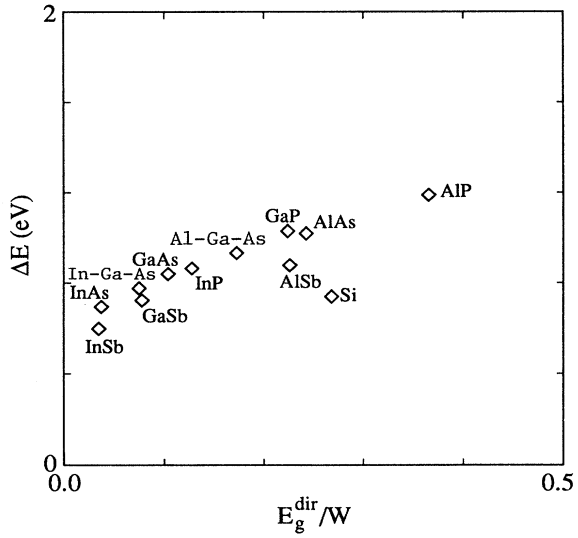

FIG. 2. The many-body corrections to the LDA direct band gaps at Γ as a function of E_g^{dir}/W, where W is the valence-band width, and E_g^{dir} is the direct band gap, for Si, nine zinc-blende-structure compounds, and two semiconductor alloys.

from the fact that in Si the lowest conduction state at Γ is p like, unlike in the other compounds where this state is s like.

Recently, much attention has been focused on developing directly a model for Σ to avoid the intensive computation effort, and to provide some better physical insight. There are two recent models[19,20] proposed for Σ which make extensive use of knowledge of the self-energy operator calculated from first principles. One is the work of Hanke and Sham[20] who construct the self-energy within the time-dependent screened Hartree-Fock approximation using a local orbital basis. The other is by Gygi and Baldereschi[19] who employ the static Coulomb-hole-plus-screened-exchange (COHSEX) approximation to the *difference* of Σ and the LDA potential. The approach of Hanke and Sham has the merits of being able to give an analytic expression for the many-body corrections to the band gaps in ionic compounds. But the $\rho^{1/3}$ model for the screening has yet to be stringently tested. Their model is still semiquantitative as it stands now, when compared to the *ab initio* results. The gaps are off by ~ 0.5 eV for diamond and LiCl. The model introduced by Gygi and Baldereschi approximates the local behavior of Σ with the LDA potential. It further uses a COHSEX model for the rest of the screening effects in Σ. It appears to work well for diamond and Si, but for Ge and some III-V compounds they examined, large discrepancies of about 0.5 eV remain to be resolved.

B. Comparison of the model and the full dielectric matrices

The *ab initio* static dielectric matrix $\epsilon^{-1}(\mathbf{q}+\mathbf{G},\mathbf{q}+\mathbf{G}',\omega=0)$ may be calculated as a ground-state property from density functional theory using the linear response approach.[6,34] Within the RPA in which the exchange correlation contributions to the screening potential are neglected, ϵ^{-1} is given by the following compact form:

$$\epsilon^{-1}_{\mathrm{RPA}}=(1-V\chi_0)^{-1}\ , \tag{8}$$

where χ_0 is the independent particle polarizability. The Adler-Wiser formulation gives[28]

$$\chi_{0,\mathbf{G},\mathbf{G}'}(\mathbf{q})=\frac{4}{\Omega}\sum_{c,v,\mathbf{k}}\frac{\langle v,\mathbf{k}|e^{-i(\mathbf{q}+\mathbf{G})\cdot\mathbf{r}}|c,\mathbf{k}+\mathbf{q}\rangle\langle c,\mathbf{k}+\mathbf{q}|e^{i(\mathbf{q}+\mathbf{G}')\cdot\mathbf{r}}|v,\mathbf{k}\rangle}{\varepsilon_{v,\mathbf{k}}-\varepsilon_{c,\mathbf{k}+\mathbf{q}}}\ . \tag{9}$$

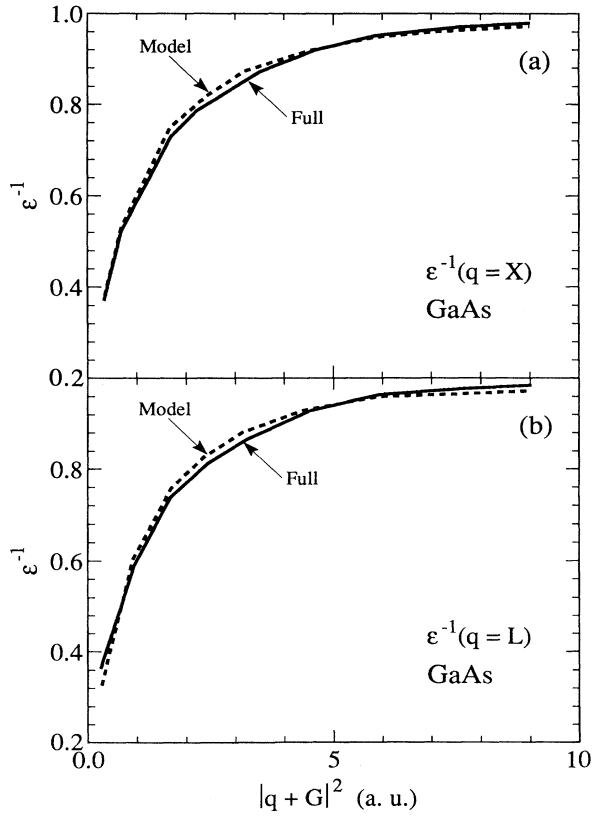

FIG. 3. (a) Comparison of the diagonal elements of the model and the RPA ϵ^{-1} for GaAs at X; (b) comparison of the diagonal elements of the model and the RPA ϵ^{-1} for GaAs at L.

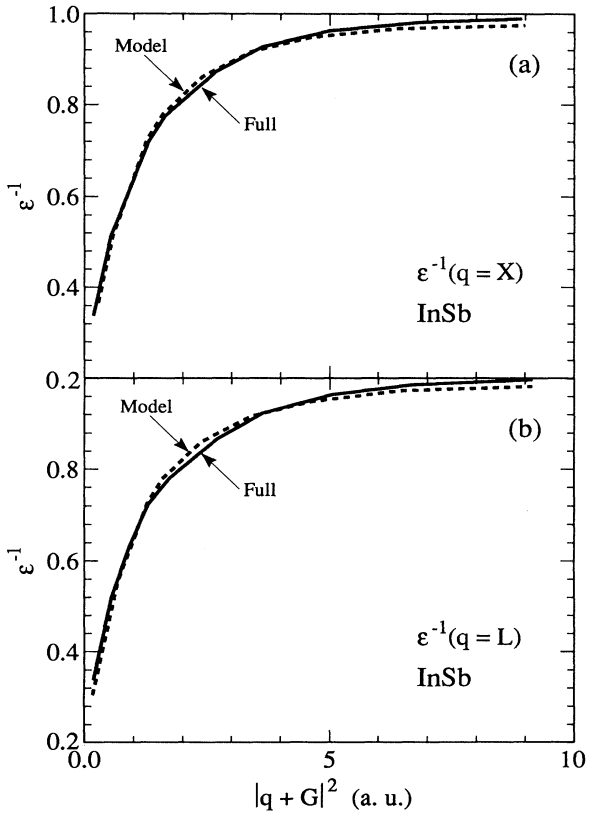

FIG. 4. (a) Comparison of the diagonal elements of the model and the RPA ϵ^{-1} for InSb at X; (b) comparison of the diagonal elements of the model and the RPA ϵ^{-1} for InSb at L.

TABLE XII. $d\Sigma/dE$ for states near the gap in LiCl. The quasiparticle energies for these states are also listed for reference.

	E_{QP} (eV)	$d\Sigma/dE$
Γ_{15v}	0.0	−0.16
Γ_{1c}	9.34	−0.14
X'_{5v}	−1.14	−0.16
X_{1c}	11.16	−0.14
L'_{3v}	−0.08	−0.18
L_{1c}	9.82	−0.13

For each $(\mathbf{q},\mathbf{G},\mathbf{G}')$, summations have to be carried out over large number of bands and $\mathbf{k}$ points. Although symmetry may be fully exploited, calculation of χ_0 is still very time consuming.

The Levine-Louie model for ϵ^{-1} that we used in the present calculation has been discussed at length in Sec. II A. The diagonal elements of ϵ^{-1} have contributions from the off-diagonal elements of ϵ, i.e., the local field effects. The inverse of the diagonal elements of ϵ^{-1} gives the macroscopic dielectric function, which is affected by the local fields. In Figs. 3 and 4, we compare the results for the diagonal elements of $\epsilon^{-1}(\mathbf{q})$ (thus with local field effects) for GaAs and InSb from the model with the *ab initio* results obtained from Eqs. (8) and (9), for $\mathbf{q}$'s at L and X. The agreement is quantitative. In the high-q region (short-range behavior in real space), the model gives a more effective screening by its nature of being from a electron gas. In the $q\rightarrow 0$ region which is not shown on these plots since the smallest $|\mathbf{q}+\mathbf{G}|$ is L or X, the *ab initio* results are expected to overestimate the screening due to the use of the LDA band structure. In the intermediate range of q, we find generally that the model screening is less effective. The behavior of the dielectric function discussed here has a direct impact on the final quasiparticle energies. Generally speaking, more effective screening corresponds to a smaller band gap.

C. The quasiparticle renormalization factor

In this section we examine an important quantity associated with the quasiparticle excitations in a solid, the renormalization factor

$$Z_{nk}=\left[1-\frac{\partial\Sigma(E)}{\partial E}\right]^{-1}_{n,\mathbf{k}}$$

for a particular state $|n,\mathbf{k}\rangle$. This quantity gives a direct measure of dynamical effects, as it is explicitly induced by the energy dependence of the self-energy operator. Static approximations to Σ, such as Hartree-Fock or COHSEX (Ref. 1), do not carry information about the interplay of a quasiparticle with the excitations (electron-hole pairs, plasmons, etc.) associated with the dynamical many-body screening effects around the quasiparticle. In the Green's-function language, Z gives the weight of the quasiparticle peak in the spectral representation. Z is directly related to the imaginary part of Σ by the following dispersion relation[1] for the quasiparticle states near the gap in a semiconductor:

$$\frac{\partial\Sigma(E_{n,\mathbf{k}})}{\partial E}=-\frac{1}{\pi}\int\frac{|\mathrm{Im}\Sigma(E')|_{n,\mathbf{k}}}{(E'-E_{n,\mathbf{k}})^2}dE' \quad (10)$$

This expression is negative definite, resulting in a less-than-unity Z. This is consistent with the fact that the quasiparticle peak can only be a part of the whole spectral function which is normalized to one.

Calculations[1,6,7,13] have shown that the exact values of Z are not sensitive to the GPP model used in the present approach. Close relationship between Z and the average charge density in a material has been pointed out by several previous papers using slightly different methods.[6,7] Table XII gives $d\Sigma/dE$ for near gap states at high symmetry points for LiCl. Table XIII gives $d\Sigma/dE$ for the highest occupied and the lowest unoccupied states at Γ for the nine zinc-blende-structure semiconductors. For the states near the gap, our calculation gives ~ -0.2 for $\partial\Sigma/\partial E$, and ~ 0.8 for Z for all the compounds listed in Table XIII. The energy dependence of Z is found to be insignificant, confirming the finding in Refs. 6 and 7. We have found Z to be state-insensitive also. These trends are tied to the fact that the energy dependence part of Σ can be well reproduced within a ~ 5-eV range of energy near the semiconductor band gap by that of a jellium with corresponding charge density.[7] Indeed, the Z values of these materials are very close to that of a jellium with $r_s\sim 2$.[1,6,7] One exception to this general observation is in LiCl which shows a Z value close to unity than the other materials. LiCl is more ionic and more localized than the rest of the materials and the static approximation applies better, thus a smaller dynamical effect.

D. The many-body correction to the VBM energy

In this subsection, we present results for the many-body corrections to the LDA energies for states at the valence-band maximum (VBM). These quantities are relevant to theories of the valence-band offsets at semiconductor interfaces.[11] In the past decade, many models

TABLE XIII. $d\Sigma/dE$ for the near gap states at Γ for nine zinc-blende-structure semiconductors.

	AlP	AlAs	AlSb	GaP	GaAs	GaSb	InP	InAs	InSb
Γ_{15v}	−0.23	−0.22	−0.23	−0.20	−0.26	−0.28	−0.26	−0.27	−0.28
Γ_{1c}	−0.24	−0.25	−0.26	−0.23	−0.27	−0.24	−0.24	−0.26	−0.25

TABLE XIV. Calculated self-energy ($\bar{\Sigma}$) and LDA exchange-correlation energy ($\overline{V_{\rm LDA}^{\rm vBH}}$) using the von Barth–Hedin exchange-correlation potential at the valence-band maximum for thirteen semiconductors. The last column is the many-body corrections to the LDA valence-band maximum energies ($\bar{\Sigma}-\overline{V_{\rm LDA}^{\rm vBH}}$). Quantities are in eV.

	$\bar{\Sigma}$	$\overline{V_{\rm LDA}^{\rm vBH}}$	$\bar{\Sigma}-\overline{V_{\rm LDA}^{\rm vBH}}$
Si	−11.90	−11.75	−0.15
Ge	−11.29	−11.31	0.02
AlP	−12.63	−12.31	−0.32
AlAs	−11.94	−11.76	−0.18
AlSb	−10.73	−10.67	−0.06
GaP	−12.55	−12.33	−0.22
GaAs	−11.83	−11.76	−0.07
GaSb	−10.66	−10.69	0.03
InP	−12.20	−10.98	−0.22
InAs	−11.52	−11.44	−0.08
InSb	−10.38	−10.38	0.00
$Al_{0.5}Ga_{0.5}As$	−11.91	−11.77	−0.14
$In_{0.53}Ga_{0.47}As$	−11.67	−11.57	−0.10

have been proposed for a unified mechanism for determining the valence-band offsets at semiconductor heterojunctions, such as the charge neutrality level model,[51] the dielectric midgap level model,[52] and the "model-solid" theory,[53] etc. However, realistic calculations[11,54,55] and recent experiments[56] indicate that these models are not completely satisfactory.

The LDA has been found to be unable to give accurate band offsets for semiconductor interfaces.[11,53] The discrepancies are more severe for the Schottky barrier heights at the metal-semiconductor interfaces,[55] where the states involved are less similar than in the valence-band offset case. As is well known, the LDA eigenvalues cannot be treated rigorously as the electron removal energies, despite the fact that the exact density functional theory would give the correct ionization energy of a solid.[57] Application of the quasiparticle theory has given excellent account for the band offset at AlAs-GaAs interface.[11] The many-body correction amounts to about 25% of the total valence-band offset in that case.[11] This fact, together with the intense experimental interest in this field, has motivated us to compute and tabulate the many-body corrections to the LDA energies of the valence-band maxima for compounds considered here. To obtain the final valence-band offset for a semiconductor interface, our data just have to be combined with a self-consistent calculation of the electrostatic potential change across the interface, which could be done within the LDA. The justification and the actual procedure for such a calculation are given in Ref. 11. By combining the valence-band results with the many-body corrections to the band gaps, one is also ready to deduce the conduction-band offsets.

As mentioned earlier, in order to make a parallel comparison between the LDA and quasiparticle results, we have used the von Barth–Hedin[37] correlation potential in the LDA calculations. In Table XIV we give $\langle {\rm VBM}|\Sigma(E_{\rm VBM}^{\rm qp})|{\rm VBM}\rangle$ and $\langle {\rm VBM}|V_{\rm LDA}^{\rm vBH}|{\rm VBM}\rangle$ and the differences between these two quantities, for Si, Ge, and nine III-VI zinc-blende structures, and the two semiconductor alloys. Since the VBM state was mainly localized on the anion, there is a clear correlation between the magnitude of the many-body correction and the properties of the anion of the material. There is also a weaker dependence on the cation. Our results reveal, as expected,[6] that the more localized the system is, the larger the correction will be. It is thus expected that the many-body corrections to the band offsets of semiconductor interfaces will be larger for II-VI compounds, which are also frequently used to form semiconductor interfaces in practice. The failure of the LDA to describe sufficiently the exchange potential, which is very influential to the VBM energies, is more severe in the more localized systems. Also we note that the many-body corrections to the LDA VBM energies for the two alloys are slightly larger in magnitude than averages of the corresponding

TABLE XV. Valence-band offsets for eight semiconductor interfaces. The LDA results here are taken from Ref. 53. The many-body correction Δ's are calculated directly from Table XIV. QP denotes the quasiparticle results obtained by adding Δ to the LDA band offsets. Results are in eV.

	LDA	Δ	QP	Expt.
AlAs-Ge	1.05	0.20	1.25	0.95[a]
GaAs-Ge	0.63	0.09	0.72	0.56[b]
AlAs-GaAs	0.37	0.11	0.48	0.55[c]
AlP-Si	1.03	0.17	1.20	
GaP-Si	0.61	0.07	0.68	0.80[d]
AlP-GaP	0.36	0.10	0.46	
InAs-GaSb	0.38	0.11	0.49	0.51[e]
AlSb-GaSb	0.38	0.09	0.47	0.45[f]

[a]Reference 58.
[b]Reference 59.
[c]Reference 60.
[d]Reference 61.
[e]Reference 62.
[f]Reference 63.

values of the constituent compounds.

We turn now to a comparison with experiments for the semiconductor interface band offsets by adding the present many-body corrections to the LDA band offset energies. The transitivity rule, which states that the valence-band offset formed at the interface of semiconductors A and B (denoted as A/B,) and at the interface of B and C (denoted as B/C) are simply related to that at A/C by $\Delta_{A/B}+\Delta_{B/C}=\Delta_{A/C}$, is found to be valid for most of the semiconductor interfaces in previous LDA calculations.[53] The addition of the many-body correction term to the LDA band offsets will of course not affect the transitivity rule. Results from self-consistent LDA calculations, which allow for the various relaxation effects, were taken from Ref. 53 for several semiconductor interfaces. The LDA calculations in Ref. 53 are moderately well converged with a theoretical uncertainty of ± 0.1 eV.[53] For AlAs-GaAs, a better converged LDA calculation gives 0.41 eV for the valence-band offset,[11] compared to 0.37 eV reported in Ref. 53. Also, much attention needs to be paid to the accuracy of the experimental results because of the technical difficulties in measuring the valence-band offsets at semiconductor interfaces.

Only lattice matched materials were considered in Ref. 53. Table XV gives the LDA band offsets,[53] the many-body corrections, the final quasiparticle band offsets, and the corresponding experimental results. A-B indicates that VBM energy in B is higher than in A. In general, the results with the many-body corrections for the valence-band offsets provide a better agreement with experiments. The largest discrepancies between theory and experiment are for AlAs-Ge and GaAs-Ge. Experimental band offsets for AlAs-Ge, GaAs-Ge, and AlAs-GaAs also show the largest violation of the transitivity rule.

The InAs-GaSb interface deserves some special attention.[64] The valence-band maximum of GaSb is located 0.49 eV higher than that of InAs, according to our calculation. The experimental value is 0.51 eV.[61] This valence-band offset is in fact larger than the direct band gap in bulk InAs. The interface system is thus in principle a metal with holes in the GaSb region and electrons in the InAs region. This is the so-called "broken gap" lineup. Our present quasiparticle calculations for both the band gap and valence-band offset provide the first *ab initio* theoretical confirmation for this interesting phenomena. If one is instead dealing with superlattices with finite thickness, this metallization does not occur until after some critical thickness is reached. For the InAs-GaSb interface (corresponding to an infinitely thick superlattice), we obtain an estimate for the overlap of the valence-band edge in GaAs and the conduction-band edge in InSb to be 0.11–0.20 eV. Experimentally it is observed to be in the vicinity of 0.15 eV.[64]

V. SUMMARY AND CONCLUSIONS

Accurate descriptions of the band structure of a wide range of semiconductors and insulators have been obtained by calculating the self-energy operator within the GW approximation of Hedin. The use of the generalized Levine-Louie model dielectric function has greatly improved the efficiency of such calculations. Satisfactory agreement between the theoretical quasiparticle energies and experimental spectroscopic data is obtained for the thirteen materials: Si, LiCl, AlP, AlAs, AlSb, GaP, GaAs, GaSb, InP, InAs, InSb, and $Al_{0.5}Ga_{0.5}As$, $In_{0.53}Ga_{0.47}As$. Our results for the many-body corrections to the LDA valence-band maximum energies should be helpful in the understanding of the valence-band offsets of semiconductor interfaces formed by these materials. The present approach has proved to be viable and accurate in calculations involving evaluation of the electron self-energy operator. Further applications to semiconductor surface are currently underway.

ACKNOWLEDGMENTS

This work was supported by NSF Grant No. DMR88-18404 and by the Director, Office of Energy Research, Office of Basic Energy Sciences, Materials Science Division of the U.S. Department of Energy under Contract No. DE-AC03-76SF00098. We thank Mark Hybertsen for a careful reading of the manuscript. X.Z. thanks Michael P. Surh for several stimulating discussions. S.G.L. acknowledges support by the J. S. Guggenheim Foundation. CRAY computer time was provided by the Office of Energy Research of the U.S. Department of Energy at the National Magnetic Fusion Energy Computer Center and at the Pittsburgh Supercomputing Center.

[1]L. Hedin, Phys. Rev. **139**, A796 (1965); L. Hedin and S. Lundqvist, in *Solid State Physics: Advances in Research and Applications,* edited by F. Seitz, D. Turnbull, and H. Ehrenreich (Academic, New York, 1969), Vol. 23, p. 1.

[2]L. J. Sham and W. Kohn, Phys. Rev. **145**, 561 (1966).

[3]M. S. Hybertsen and S. G. Louie, Comments Cond. Mat. Phys. **13**, 223 (1987).

[4]G. Strinati, H. J. Mattausch, and W. Hanke, Phys. Rev. Lett. **45**, 290 (1980); Phys. Rev. B **25**, 2867 (1982); W. Hanke, Th. Golzer, and H. J. Mattausch, Solid State Commun. **51**, 23 (1984).

[5]C. S. Wang and W. E. Pickett, Phys. Rev. Lett. **51**, 597 (1983); Phys. Rev. B **30**, 4719 (1984).

[6]M. S. Hybertsen and S. G. Louie, Phys. Rev. Lett. **55**, 1418 (1985); Phys. Rev. B **34**, 5390 (1986).

[7]R. W. Godby, M. Schlüter, and L. J. Sham, Phys. Rev. Lett. **56**, 2415 (1986); Phys. Rev. B **36**, 6497 (1987); **37**, 10 159 (1988).

[8]S. B. Zhang, D. Tománek, M. L. Cohen, S. G. Louie, and M. S. Hybertsen, Phys. Rev. B **40**, 3162 (1989).

[9]M. S. Hybertsen and S. G. Louie, Phys. Rev. Lett. **58**, 1551 (1987); Phys. Rev. B **38**, 4033 (1988). Also see R. S. Becker, B. S. Swartzentruber, J. S. Vickers, M. S. Hybertsen, and S. G. Louie, Phys. Rev. Lett. **60**, 116 (1988).

[10]X. Zhu, S. B. Zhang, S. G. Louie, and M. L. Cohen, Phys. Rev. Lett. **63**, 2112 (1989).

[11]S. B. Zhang, D. Tománek, S. G. Louie, M. L. Cohen, and M. S. Hybertsen, Solid State Commun. **66**, 585 (1988).

[12]M. S. Hybertsen and M. Schlüter, Phys. Rev. B **36**, 9683 (1987); S. B. Zhang, M. S. Hybertsen, M. L. Cohen, S. G. Louie, and D. Tománek, Phys. Rev. Lett. **63**, 1495 (1989).
[13]J. E. Northrup, M. S. Hybertsen, and S. G. Louie, Phys. Rev. Lett. **59**, 819 (1987); Phys. Rev. B **39**, 8198 (1989); M. P. Surh, J. E. Northrup, and S. G. Louie, *ibid.* **38**, 5976 (1988).
[14]P. Hohenberg and W. Kohn, Phys. Rev. **136**, B864 (1964); W. Kohn and L. J. Sham, *ibid.* **140**, A1133 (1965).
[15]S. G. Louie, in *Electronic Structure, Dynamics and Quantum Structural Properties of Condensed Matter,* edited by J. Devreese and P. van Camp (Plenum, New York, 1985), p. 335.
[16]For systems with a gap in the excitation spectrum, see J. P. Perdew, R. G. Parr, M. Levy, and J. L. Balduz, Jr., Phys. Rev. Lett. **49**, 1691 (1982); J. P. Perdew and M. Levy, *ibid.* **51**, 1884 (1983); L. J. Sham and M. Schlüter, *ibid.* **51**, 1888 (1983).
[17]For metallic systems, see K. Schönhammer and O. Gunnarsson, Phys. Rev. B **37**, 3128 (1988); D. Mearns, *ibid.* **38**, 5906 (1988).
[18]F. Bechstedt and R. Del Sole, Phys. Rev. B **38**, 7710 (1988); (unpublished).
[19]F. Gygi and A. Baldereschi, Phys. Rev. Lett. **62**, 2160 (1989).
[20]W. Hanke and L. J. Sham, Phys. Rev. B **38**, 13 361 (1988).
[21]M. S. Hybertsen and S. G. Louie, Phys. Rev. B **37**, 2733 (1988).
[22]Z. H. Levin and S. G. Louie, Phys. Rev. B **25**, 6310 (1982).
[23]*Zahlenwerte und Funkionen aus Naturwissenschaften und Technik,* edited by U. Madelung, M. Schultz, and H. Weiss, Landolt-Börnstein, New Series, Vol. III, Pt. 17a and 22a (Springer-Verlag, Berlin, 1982).
[24]G. Baldini and B. Bosacchi, Phys. Status Solidi **38**, 325 (1970).
[25]R. T. Poole, J. G. Jenkin, R. C. G. Leckey, and J. Liesegang, Chem. Phys. Lett. **22**, 101 (1973); L. I. Johnsson and S. B. H. Hagstrom, Phys. Scr. **14**, 55 (1976).
[26]L. Ley, R. A. Pollak, F. R. McFeely, S. P. Kowalczyk, and D. A. Shirley, Phys. Rev. B **9**, 600 (1974).
[27]D. E. Eastman, W. D. Grobman, J. L. Freeouf, and M. Erbudak, Phys. Rev. B **9**, 3473 (1974).
[28]S. D. Adler, Phys. Rev. **126**, 413 (1962); N. Wiser, *ibid.* **129**, 62 (1963).
[29]See, for example, G. D. Mahan, *Many-Particle Physics* (Plenum, New York, 1981).
[30]J. Lindhard, K. Dan. Vidensk. Selsk. Mat. Fys. Medd. **28**, (8), 1 (1954).
[31]J. Hubbard, Proc. R. Soc. London Ser. A **243**, 336 (1957).
[32]K. S. Singwi, M. P. Tosi, R. H. Land, and A. Sjölander, Phys. Rev. **176**, 589 (1968); K. S. Singwi, A. Sjölander, M. P. Tosi, and R. H. Land, Phys. Rev. B **1**, 104 (1970).
[33]J. P. Walter and M. L. Cohen, Phys. Rev. B **2**, 1821 (1970); **5**, 3101 (1972).
[34]S. Baroni and R. Resta, Phys. Rev. B **33**, 7107 (1986); M. S. Hybertsen and S. G. Louie, *ibid.* **35**, 5585 (1987); **35**, 5602 (1987); Z. H. Levine and D. C. Allan, Phys. Rev. Lett. **63**, 1719 (1989).
[35]D. R. Hamann, M. Schlüter, and C. Chiang, Phys. Rev. Lett. **43**, 1494 (1979); L. Kleinman, Phys. Rev. B **21**, 2630 (1980); G. B. Bachelet and M. Schlüter, *ibid.* **25**, 2103 (1982).
[36]D. M. Ceperley and B. J. Adler, Phys. Rev. Lett. **45**, 566 (1980), as parametrized by J. P. Perdew and A. Zunger, Phys. Rev. B **23**, 5048 (1981).
[37]U. von Varth and L. Hedin, J. Phys. C **5**, 1629 (1972).
[38]J. A. Van Vechten and T. K. Bergstresser, Phys. Rev. B **1**, 3351 (1970).
[39]A.-B. Chen and A. Sher, Phys. Rev. Lett. **40**, 900 (1978).
[40]K. C. Hass, R. J. Lempert, and H. Ehrenreich, Phys. Rev. Lett. **52**, 77 (1984).
[41]J. Hwang, P. Pianetta, Y.-C. Pao, C. K. Shih, Z.-X. Shen, and P. A. P. Lindberg, Phys. Rev. Lett. **61**, 877 (1988); A. Zunger, S.-H. Wei, L. G. Ferreira, and J. E. Bernard, *ibid.* **65**, 353 (1990); S.-H. Wei, L. G. Ferreira, J. E. Bernard, and A. Zunger, Phys. Rev. B **42**, 9622 (1990).
[42]M. S. Hybertsen and S. G. Louie, Phys. Rev. B **34**, 2920 (1986).
[43]M.-F. Li, M. P. Surh, and S. G. Louie, in *Proceedings of the 19th International Conference of the Physics of Semiconductors,* edited by W. Zawadzki (Institute of Physics, Warsaw, Poland, 1988), Vol. II, p. 857; M. P. Surh, M.-F. Li, and S. G. Louie, Phys. Rev. B **43**, 4286 (1991).
[44]M. L. Cohen and J. R. Chelikowski, *Electronic Structure and Optical Properties of Semiconductors* (Springer-Verlag, Berlin, 1988).
[45]J. R. Chelikowski and M. L. Cohen, Phys. Rev. B **14**, 556 (1976).
[46]B. Monemar, Phys. Rev. B **8**, 5711 (1973).
[47]H. J. Lee, L. Y. Juravel, J. C. Woolley, and A. J. SpringerThorpe, Phys. Rev. B **21**, 659 (1980).
[48]A. Joullie, B. Girault, A. M. Joullie, and A. Zien-Eddine, Phys. Rev. B **25**, 7830 (1982).
[49]C. A. Mead and W. G. Spitzer, Phys. Rev. Lett. **11**, 358 (1965).
[50]K. Alavi, R. L. Aggarwal, and S. H. Groves, Phys. Rev. B **21**, 1311 (1980).
[51]J. Tersoff, Phys. Rev. B **30**, 4874 (1984).
[52]M. Cardona and N. E. Christensen, Phys. Rev. B **35**, 6182 (1987).
[53]C. G. Van de Walle and R. M. Martin, Phys. Rev. B **35**, 8154 (1987); C. G. Van de Walle, *ibid.* **39**, 1871 (1989).
[54]M. S. Hybertsen, Phys. Rev. Lett. **64**, 555 (1990).
[55]G. P. Das, P. Blöchl, O. K. Andersen, N. E. Christensen, and O. Gunnarsson, Phys. Rev. Lett. **63**, 1168 (1989).
[56]D. R. Heslinga, H. H. Weitering, D. P. van der Werf, T. M. Klapwijk, and T. Himba, Phys. Rev. Lett. **64**, 1589 (1990).
[57]C.-O. Almbladh and U. von Barth, Phys. Rev. B **31**, 3231 (1985).
[58]M. K. Kelly, D. W. Niles, E. Colavita, G. Margaritonmdo, and M. Henzler (unpublished), as quoted in G. Margaritondo, Phys. Rev. B **31**, 2526 (1985).
[59]J. P. Waldrop, E. A. Kraut, S. P. Kowalczyk, and R. W. Grant, Surf. Sci. **132**, 513 (1983).
[60]J. Batey and S. L. Wright, J. Appl. Phys. **59**, 200 (1986).
[61]P. Perfetti, F. Patella, F. Sette, C. Quaresima, C. Capasso, A. Savioa, and G. Margaritondo, Phys. Rev. B **30**, 4533 (1984).
[62]J. Sakaki, L. L. Chang, R. Ludeke, C.-A. Chang, G. A. Sai-Halasz, and L. Esaki, Appl. Phys. Lett. **31**, 211 (1977).
[63]J. Menéndez and A. Pinczuk (unpublished), as quoted by Van de Walle and Martin in Ref. 53.
[64]L. L. Chang and L. Esaki, Surf. Sci. **98**, 70 (1980).